GEOSTANDARDS and
GEOANALYTICAL
RESEARCH

Sn Isotopic Values in Ten Geological Reference Materials by Double-Spike MC–ICP-MS

Zhao-Yang **Wang** (1, 2, 3), Zhen-Yu **Luo** (1, 2), Le **Zhang** (1, 2) (iD), Jun-Jie **Liu** (1, 2) and Jie **Li** (1, 2)* (iD)

(1) State Key Laboratory of Isotope Geochemistry, Guangzhou Institute of Geochemistry, Chinese Academy of Sciences, Guangzhou 510640, China
(2) CAS Centre for Excellence in Deep Earth Science, Guangzhou 510640, China
(3) College of Earth and Planetary Sciences, University of Chinese Academy of Sciences, Beijing 100101, China
* Corresponding author. e-mail: jieli@gig.ac.cn

The tin mass fraction and the $\delta^{120/118}$Sn relative to NIST SRM 3161a were measured for ten geological reference materials among which the Sn isotopic values of W-2a, JA-2, JG-2, G-2, GBW07316, NOD-A-1 and SGR-1 are reported for the first time. The sample preparation procedure implemented in this study was based on acid digestion and matrix separation by two-stage chromatographic using AG-MP-1 and TRU-Spec resin. Isotopic measurements were carried out by multi-collector inductively coupled plasma-mass spectrometry (MC–ICP-MS), using a ^{117}Sn–^{119}Sn double-spike technique to correct for the instrumental mass fractionation effects. The overall precision of this method is estimated to be $\pm$ 0.03‰ (2s, n = 81) and $\pm$ 0.07‰ (2s, n = 6) for the NIST SRM 3161a and a geological reference material BHVO-2, respectively.

Keywords: double-spike, geological reference materials, MC–ICP-MS, Sn isotopes, two-stage ion-exchange chromatography.

Tin, a moderately siderophile, chalcophile and volatile element, has ten naturally occurring stable isotopes. The isotopic signature of Sn has been used to investigate the magmatic sources, the differentiation of terrestrial rocks and meteorites (Badullovich *et al.* 2017, Wang *et al.* 2018, Yao *et al.* 2018, Qu *et al.* 2020), and the formation and differentiation of celestial bodies in the early history of the Solar System (Wang *et al.* 2018, Creech *et al.* 2019, Creech and Moynier 2019, Wang *et al.* 2019). Tin isotopic analysis has also been employed to determine the provenance of raw materials in ancient bronze and identify fakes consisting of bronze in archaeology (Haustein *et al.* 2010, Nickel *et al.* 2012, Yamazaki *et al.* 2014, Brügmann *et al.* 2017, Schulze *et al.* 2017, Berger *et al.* 2018, Mason *et al.* 2020). The influence of Sn on the environment can also be studied through the measurement of Sn isotopes (Encinar *et al.* 2002, Malinovskiy *et al.* 2009).

Tin is a trace element in igneous rocks and sedimentary materials. It has an atomic mass range from 112 to 124. During isotopic measurement, this mass range results in isobaric interference from elements such as Cd, In, Te and Xe (Table 1), and polyatomic interference from the plasma source (Table S1), such as Ar$_3$, ArGe, ArAs, ArSe, MoN, MoO, RuO, RuN and PdO (Wang *et al.* 2017, Friebel *et al.* 2020). The sample matrix may also affect the Sn isotopic analysis. Thus, separating Sn cleanly from samples is crucial to perform precise and accurate Sn isotope measurements.

Ion-exchange chromatography has been widely applied in the separation of Sn from geological samples in recent decades (de Laeter and Jeffery 1965, 1967, McNaughton and Rosman 1991). The TRU-Spec resin has been used to separate Sn recently (Yi *et al.* 1995, Nickel *et al.* 2012, Balliana *et al.* 2013, Yamazaki *et al.* 2013, Brügmann *et al.* 2017, Creech *et al.* 2017); however, it could not separate some matrix elements cleanly, such as In, Mo, Tl and Bi (Wang *et al.* 2017). A three-stage ion-exchange chromatography with AG1-X8 resin has also been designed to purify Sn (Wang *et al.* 2017); however, it is complicated and time-consuming. More recently, a three-stage column procedure based on three different kinds of resin, AG1-X8, TRU-Spec resin and Pre-filter resin, a has

GEOSTANDARDS and GEOANALYTICAL RESEARCH

Table 1.
Potential interferences on Sn isotopes

	112	113	114	115	116	117	118	119	120	121	122	123	124
Sn	0.97		0.65	0.34	14.5	7.7	24.2	8.6	32.6		4.6		5.8
Cd	24.1	12.2	28.7	7.5									
In		4.3		95.7									
Sb										57.4		47.6	
Te									0.1		2.6	0.91	4.8
Xe													0.09

The relative abundances of isotope are shown as a percentage and the data are from Rosman and Taylor (1998).
Molecular interferences are shown in Table S1.

been applied (Friebel *et al.* 2020). This procedure yields highly pure Sn solutions and is relatively simple. Friebel *et al.* (2020) applied internal normalisation to correct for the isotopic fractionation instead of double-spike (DS). However, mass fraction of Sn in natural samples could not be achieved in such a way.

Measurement of Sn isotopes by thermal ionisation mass spectrometer (TIMS) has been carried out since the 1960s (de Laeter and Jeffery 1965, 1967). However, the high ionisation potential (~ 7.34 eV) of Sn leads to low ion beam intensities, unstable ionisation and time-dependent instrumental mass fractionation. Although instrumental mass fractionation can be corrected by DS and ion beam intensities can be improved by ionisation enhancer, a precision of only 0.06‰ (per mass unit, 2s) could be achieved for Sn isotopic analyses by TIMS (Rosman and McNaughton 1987, McNaughton and Rosman 1991). With the development of multi-collector inductively coupled plasma-mass spectrometry (MC-ICP-MS), these shortcomings have been overcome (Clayton *et al.* 2002, Creech *et al.* 2017, Wang *et al.* 2017, Friebel *et al.* 2020).

Based on the previous studies, a chemical separation protocol has been developed in this study utilising two-stage column separation with AG MP-1 anion exchange and TRU-Spec resin. The Sn mass fraction and isotopic compositions were determined by ^{117}Sn–^{119}Sn DS technique and MC-ICP-MS. The δ^{120}Sn/^{118}Sn$_{NIST\ SRM\ 3161a}$ was chosen to express Sn isotopic composition. The Sn mass fractions and isotopic compositions for ten geological reference materials have been analysed in this study. The matrices of these reference materials vary greatly, including igneous rocks from basic to acidic and sedimentary materials. There has been barely any Sn isotopic signature data for geological reference materials reported before this study. This study aims to facilitate inter-laboratory comparison of high-precision Sn mass fractions and isotopic data.

Experimental procedure

Reagents and materials

The hydrochloric acid (HCl), hydrofluoric acid (HF) and nitric acid (HNO$_3$) were purified by DST-1000 sub-boiling stills (Savillex Corporation, USA). All the acids were diluted to appropriate concentrations by ultrapure water (Milli-Q, resistivity of 18.2 MΩ cm). The AG MP-1 (100–200 mesh) anion-exchange resin is from Bio-Rad Laboratories (Hercules, CA, USA). The TRU-Spec (100–200 mesh) resin is from Eichrom Technologies Inc. (Darien, IL, USA). A synthetic multi-element solution containing sixty-eight elements with a concentration of 1 μg ml^{-1} was prepared from the AccuStandard containing fluoride soluble elements (MISA 05-1), rare earth metals (MISA 01-1), transition metals (MISA 06-1), alkaline earth elements (MISA 04-1) and precious metals (MISA 02-1) to facilitate the optimisation of the column separation parameters. The NIST SRM 3161a (Lot No. 070330) was adopted as the Sn isotope standard solution. Another Sn standard solution from China Iron and Steel Research Institute Group, NCS Sn (Lot GSBG62042-90), was utilised to verify the functionality of this measurement procedure. The ^{117}Sn–^{119}Sn DS was from the Oak Ridge National Laboratory, USA.

Double-spike design

Double-spike is a precise method for the correction of mass fractionation during mass spectrometry for elements with more than three isotopes. This technique can acquire the contents of the elements of interest while correcting the instrument fractionation (Dodson 1963, Eugster *et al.* 1969, Russell *et al.* 1978, Creech *et al.* 2017, Hu and Dauphas 2017, Wang *et al.* 2017, Zhang *et al.* 2018).

To calibrate mass fractionation during Sn isotopic analysis and achieve precise Sn isotopic composition and mass fractions, we selected to use a ^{117}Sn–^{119}Sn DS

following a procedure reported by Zhang *et al.* (2018). ^{117}Sn-^{118}Sn-^{119}Sn-^{120}Sn are employed for the DS inversion using an iterative Newton Raphson procedure Albarède and Beard (2004) with the detailed in Zhang *et al.* (2015). The ^{120}Te is the only elemental isobaric interference on tin isotopes in this inversion procedure. In previously studies, ^{117}Sn and ^{122}Sn were elected to produce the DS solution (Creech *et al.* 2017, Wang *et al.* 2017), using a ^{117}Sn-^{118}Sn-^{122}Sn-^{124}Sn and a ^{116}Sn-^{117}Sn-^{122}Sn-^{124}Sn inversion, respectively. Compared with ^{117}Sn-^{122}Sn, ^{117}Sn–^{119}Sn have less isobaric interference. Although using a ^{117}Sn-^{122}Sn DS has minimum theoretical errors according to the Double Spike Toolbox of Rudge *et al.* (2009), the difference in theoretical errors between these hypothetical DS options is smaller than our analytical uncertainties (Figure S1).

Sample preparation and digestion

All digestions and separations were performed in a Class 100 clean laboratory at the State Key Laboratory of Isotope Geochemistry, Guangzhou Institute of Geochemistry, Chinese Academy of Science (GIG-CAS), Guangzhou, China. PTFE beakers were used for all samples and solutions. These beakers were previously cleaned with concentrated HNO_3 and HCl (AR grade) and soaked overnight in 7 mol l^{-1} purified HNO_3 at ~ 120 °C and rinsed with ultrapure water three times. Approximately 50–100 mg of sample powder and a corresponding amount of ^{117}Sn–^{119}Sn DS were weighed in Teflon beakers (the mass fraction of DS is 50–60% in the DS-sample mixture of Sn, the acceptable DS proportion relative to the sample range from 0.2 to 0.8 by Zhang *et al.* (2018)). The samples were digested with 1 ml of concentrated HNO_3 and 2 ml HF on a hotplate at 120 °C for at least 72 h. After digestion, the solutions were evaporated to dryness at 120 °C. Subsequently, the residue was dissolved in 1 ml 6 mol l^{-1} HCl. Then, all samples were evaporated to dryness at 120 °C. Finally, these samples were dissolved in 2 ml 1 mol l^{-1} HCl and heated on a hot plate at 120 °C for 12 h before the chemical separation.

Two-stage column separation

A two-stage column separation with anion-exchange chromatography (AG MP-1) and TRU-spec resin was used to separate Sn from geological materials. The separation processes are shown in Table 2.

For the first stage, 2 ml of AG MP-1 resin was filled in a 4 ml column (Bio-Rad Laboratories, with ~ 0.8 cm inner diameter and ~ 4 cm high resin bed) and pre-cleaned

Table 2.
Separation processes in this study

Resin	Resin volume (ml)	Step	Eluant volume (ml)	Purpose
AG-MP-1	2.00	1 mol l^{-1} HCl	4	Condition
		1 mol l^{-1} HCl	2	Loading
		1 mol l^{-1} HCl	12	Matrix removal
		1 mol l^{-1} HNO_3	4	Collection of Sn
TRU-Spec	0.15	1 mol l^{-1} HCl	2	Condition
		1 mol l^{-1} HCl	0.2	Loading
		1 mol l^{-1} HCl	8	Matrix removal
		0.4 mol l^{-1} HNO_3	6	Collection of Sn

three times with 6 ml of 6 mol l^{-1} HNO_3 and 6 ml of high-purity (Milli-Q) water. The resin was subsequently conditioned with 4 ml of 1 mol l^{-1} HCl. Samples in 2 ml of 1 mol l^{-1} HCl were loaded on the columns and washed with 12 ml of 1 mol l^{-1} HCl, enabling elution of several isobaric interferences of Sn and complex matrix elements. The next step was the elution of Sn with 4 ml 1 mol l^{-1} HNO_3 and evaporation of the solutions to dryness at 120 °C. Subsequently, 0.2 ml 6 mol l^{-1} HCl was added to the samples and they were dried on a hotplate at 120 °C. Finally, these samples were taken up in 0.2 ml 1 mol l^{-1} HCl and were then ready for the next column separation stage.

For the second stage, 0.15 ml TRU-Spec resin was filled in a Bio-Spin chromatography column (0.4 cm inner diameter, 3.5 cm resin bed height) and then cleaned with three rounds of alternating 2 ml of 0.4 mol l^{-1} HNO_3 solutions and 2 ml Milli-Q water. The resin was then conditioned with 2 ml 1 mol l^{-1} HCl. The samples were loaded onto the columns in 0.2 ml of 1 mol l^{-1} HCl and eluted with 8 ml 1 mol l^{-1} HCl. Subsequently, the Sn was eluted with 6 ml 0.4 mol l^{-1} HNO_3. Concentrated HF (2 μl) was added to each solution. The samples were evaporated at 120 °C and then diluted to 0.5 ml with high-purity water before being analysed by MC-ICP-MS.

Mass spectrometry measurements

Element concentration was determined using a quadrupole ICP-MS (Thermo Scientific Xseries-2). Ion lens settings, nebuliser gas and make-up gas flow rates were optimised for good signal intensities for Ir and Ce. A typical sensitivity of ~ 3×10^4 cps ng^{-1} for ^{193}Ir and an oxide production rate of ~ 1.2% for the CeO$^+$/Ce$^+$ ratio have been achieved. Drift corrections were carried out using Ir as an internal standard and by repeatedly analysing a quality control solution as a drift monitor over the duration of a run.

Table 3.
Typical instrumental set up for MC-ICP-MS measurements in this study (operating conditions have been reported previously by Zhang *et al.* 2018)

Parameter	Value
RF power	1180 W (optimised daily)
Auxiliary gas (Ar) flow rate	0.98 l min^{-1} (optimised daily)
Sample gas (Ar) flow rate	0.975 l min^{-1} (optimised daily)
Cooling gas (Ar) flow rate	16.00 l min^{-1}
Measurement mode	Static
Interface cones	H sample cone + X skimmer cone (nickel)
Acceleration voltage	10 kV
Detection system	Faraday cups
Amplifier	10^{11} Ω
Integration time	4.19 s
Mass resolution	~ 400 (low)
Nebuliser	MicoFlow PFA-50; speed: ~ 50 µl min^{-1}
Spray chamber	Dual cyclonic-Scott (quartz)

Cup configuration	L4 ^{116}Sn	L3 ^{117}Sn	L2 ^{118}Sn	L1 ^{119}Sn	C ^{120}Sn	H1	H2 ^{122}Sn	H3 ^{124}Sn	H4

Isotopic analyses of Sn for all samples were performed using a Thermo Fisher Scientific Neptune Plus MC-ICP-MS instrument at the State Key Laboratory of Isotope Geochemistry, Guangzhou Institute of Geochemistry, Chinese Academy of Sciences (GIGCAS), Guangzhou, China. The typical instrumental setup during MC-ICP-MS analysis is shown in Table 3. Sample solutions were introduced into the plasma using a self-aspiration PFA nebuliser (~ 50 µg min^{-1}) and a quartz dual cyclonic-Scott spray chamber. The isotope measurements were performed in static mode at a low mass resolution (~ 400, the mass resolution was determined by $R = M/W_{0.05}$, where R is mass resolution, M is (120 + 119)/2, and the $W_{0.05}$ is the peak width at 5% of the peak height of ^{120}Sn). In previous studies, the dry-plasma condition was used to measure the Sn isotopic compositions (Creech *et al.* 2017, Wang *et al.* 2017), which can improve the sensitivity of MC-ICP-MS, but the Aridus™ desolvator system in our laboratory would produce a notable memory effect, and further result in the instability of the instrument.

Before measurement, samples and standard solutions were diluted to Sn concentration of ~ 100 µg ml^{-1} by 2% HNO$_3$–0.01%HF. The typical signal with this set up on ^{120}Sn was ~ 2 V. The standard solution (NIST SRM 3161a) was analysed five times to check the instrument's stability. The NIST SRM 3161a was analysed after each batch of three to five samples during sample solution measurement. Each analysis included sixty cycles of 4.2 s integration time. The injection system was washed between each of the measurements with 2% HNO$_3$ and 2% HNO$_3$ + 0.01% HF achieving ^{120}Sn signals of < 0.5 mV. The signal of 2% HNO$_3$ + 0.01% HF was periodically measured and used for the background correction.

To report mass-dependent Sn isotope fractionation, the Sn isotope amount ratios are stated in delta notation, including $\delta^{122/118}$Sn$_{Sn\_IPGP}$ (Creech *et al.* 2017), and $\delta^{124/116}$Sn$_{NIST\ 3161a}$ (Wang *et al.* 2017). Here we choose $\delta^{120/118}$Sn$_{NIST\ SRM\ 3161a}$ to express Sn isotopic signature, because ^{118}Sn and ^{120}Sn have the highest abundance in Sn isotopes and the lesser isobaric interference.

The delta notation is expressed as:

$$\delta^{120/118}Sn = \left[\frac{\left(^{120}Sn/^{118}Sn\right)_{sample}}{\left(^{120}Sn/^{118}Sn\right)_{standard}} - 1 \right] \qquad 1$$

where $(^{120}Sn/^{118}Sn)_{sample}$ and $(^{120}Sn/^{118}Sn)_{standard}$ are the isotopic ratios of ^{120}Sn/^{118}Sn for the sample and the standard solution, respectively. In the absence of a universal standard solution, most laboratories choose NIST SRM 3161a to compare Sn isotopic data from different laboratories. This study also selected NIST SRM3161a (Lot No. 070330) as the standard solution assume that it has consistent isotopic composition between lots. For natural samples, NIST SRM 3161a was selected as the zero-delta standard solution for delta notation of Sn isotopic data. It is suggested here that NIST SRM 3161a should be served as a common reference material to allow inter-laboratory comparisons of Sn isotopic reference materials and geological samples.
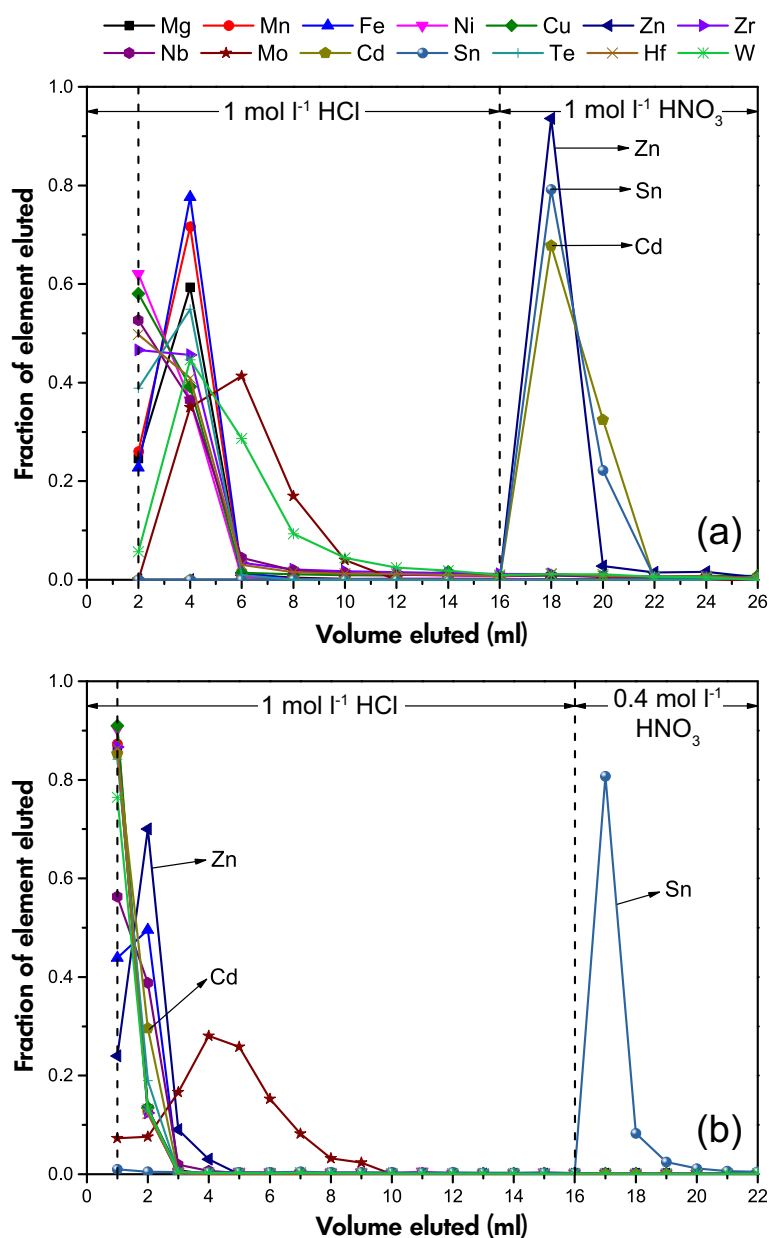
Figure 1. Elution curves of Sn separation for a synthetic multi-element solution. (a) The separation curve of the AG-MP-1 resin; (b) the elution curve of the TRU-Spec resin. All the load solutions are a synthetic multi-element solution with a concentration of 1 μg ml^{-1} in 1 mol l^{-1} HCl, and the volumes are 2 and 1 ml, respectively.

Results and discussion

Optimisation of the two-stage chromatography

To achieve accurate isotopic compositions by MC-ICP-MS, the target elements need to be isolated to reduce the interference from the matrix elements, especially Fe, Mn, Zn, Mo, Cd, In and Te, which create matrix effects and isobaric interference with Sn, but are unable to be resolved by MC-ICP-MS mass resolution (Fehr *et al.* 2004). In the first column

separation stage of this study, most of matrix elements were separate by using AG MP-1 resin, and in the second stage, Sn was further purified with TRU-Spec resin from other elements that create isobaric interference, such as Cd. The elution behaviour of Sn and matrix elements was examined using a synthetic multi-element solution (with a concentration of 1 μg ml^{-1}).

Previous studies have shown that AG MP-1 is a strong anion-exchange resin that can efficiently remove most matrix

Table 4.
Ratios of element X relative to Sn mass fractions after separation of GSP-2 and NOD-A-1

[X]/[Sn]									
	Mn	**Fe**	**Cu**	**Zn**	**Ge**	**Mo**	**Cd**	**Te**	**U**
GSP-2	0.00002	0.00004	0.00017	0.00018	0.00002	0.0005	0.00035	0.00033	$< 1 \times 10^{-5}$
NOD-A-1	0.00063	0.00124	0.00055	0.00072	0.00053	0.00086	0.00065	0.00053	$< 1 \times 10^{-5}$

elements from complex geological samples in HCl solution, such as alkalis, alkaline earth metals, Mn and Ti (van der Walt and Coetzee 1996, Sun *et al.* 2012, Cheng *et al.* 2014, Lamboux *et al.* 2020). The AG MP-1 resin has a strong adsorption capacity for Sn in the form of $SnCl_6^{2-}$ in concentrated HCl medium. The effect of HCl concentration on the elution behaviour of AG MP-1 resin was evaluated with an aliquot of 2 ml of the synthetic multi-element solution. The results show that for solutions with 1 mol l^{-1} HCl concentration, Sn, Zn and Cd are completely adsorbed on the resin. While Fe, Mg, Mn, Ni, Cu, Nb, Te and W are easily removed. Sn, Zn and Cd could be extracted with a 0.5 mol l^{-1} HNO_3 solution (Figure 1). In this step, the recovery of Sn is > 99%. The AG MP-1 resin is preferred over AG1-X8 for the separation of matrix elements as it has a greater adsorption capacity and requires less volume of elution acid. At this stage, Cd and Zn are unable to be separated, yet may cause serious interference in MC-ICP-MS analysis. Therefore, a second stage of column separation is required.

After separation of Sn from a 1 ml of synthetic multi-element solution by TRU-Spec resin, the matrix elements, such as Mn, Fe, Ni, Cu, Zn, Nb, Cd, Te and W, were not retained on the TRU-Spec resin in 1 mol l^{-1} HCl medium (Figure 1). This is consistent with a prior study (Balliana *et al.* 2013). Sn could be collected by 0.4 mol l^{-1} HNO_3 solution. In this step, the recovery of Sn is ~ 92.7%.

The suitability of this chromatography procedure was verified using geological reference materials GSP-2 and NOD-A-1. The ratios of an element X calibrated to the Sn concentration are reported in Table 4, indicating that the [X]/[Sn] ratios are always < 0.002. The two-stage chromatography has > 90% Sn recovery, which means that this method is quite efficient in purifying Sn from the complex matrix.

Measurement precision

The repeatability of the whole measurement procedure was evaluated by repeated analyses of two Sn standard solutions: NIST SRM 3161a and the China Iron and Steel Research Institute Group Sn standard solution (NCS). The long-term mean $\delta^{120/118}Sn_{SRM\ 3161a}$ for the NIST SRM 3161a Sn solution over 6 months was 0.00 ± 0.03‰ (2s, n = 81, Figure 2). Previous laboratory studies on the use of NIST SRM 3161a to spike aliquots have reported $\delta^{120/118}Sn$ of
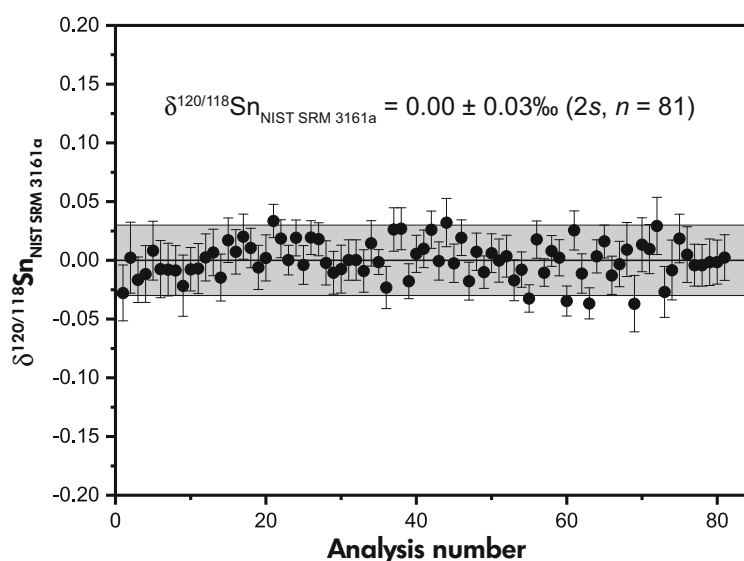
Figure 2. Repeatability on measurements of standard solution NIST SRM 3161a (n = 81). Range bars are the measurement uncertainties (2SE), and the measurement repeatability is represented by the grey band (2s).

0.00 ± 0.02‰ (2s, n = 9; Wang et al. 2017). These results indicate that the measurements from this study are sufficiently precise.

The Sn isotopic composition of another standard solution, Sn NCS, was also determined. The DS and standard sample bracketing (SSB) methods were both adopted to correct for the instrumental mass fractionation. The $\delta^{120/118}Sn_{\text{NIST SRM 3161a}}$ values of NCS are -0.09 ± 0.05‰ (2s, n = 17) and -0.11 ± 0.02‰ (2s, n = 7), respectively (Figure 3). These results demonstrate the consistency between these two different technologies on mass fractionation correction and that the DS made up of ^{117}Sn–^{119}Sn is able to correct for the instrumental mass fractionation and obtain satisfactory results.
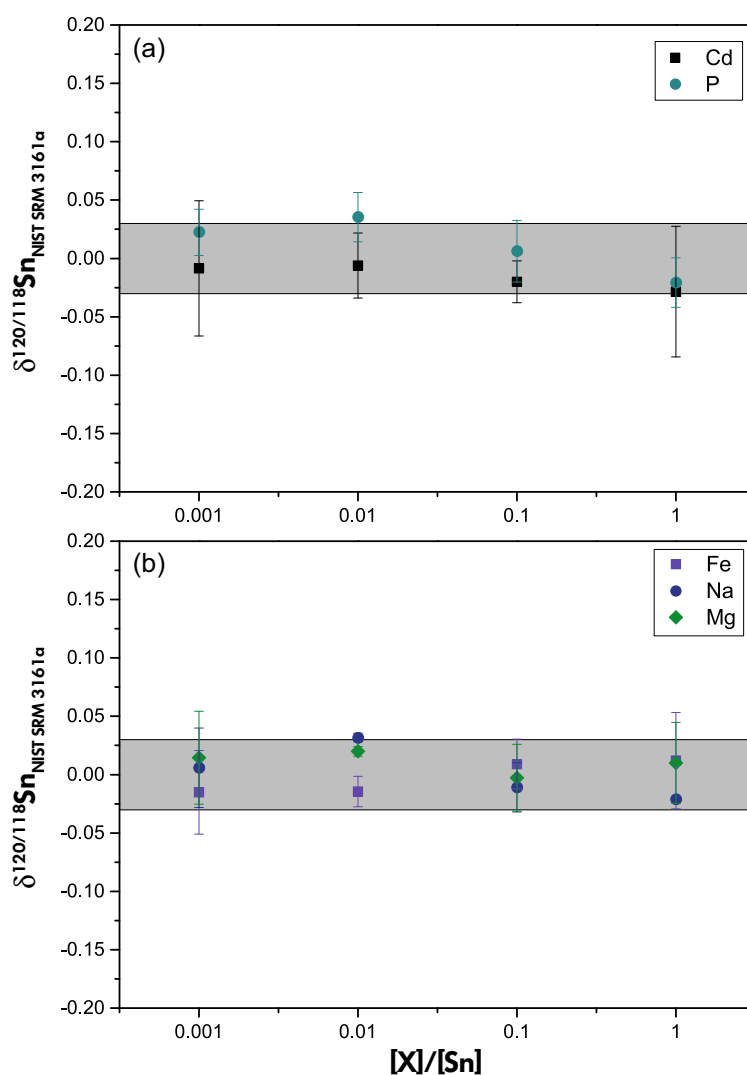
The NIST SRM 3161a reference material was doped with different elements (Cd, P, Na, Mg and Fe) in varying mass fractions relative to Sn ([X]/[Sn] = 0.001–1) to test the matrix effects. The results show that these elements at proportions up to [X]/[Sn] of 1 do not affect the measurement (Figure 4).

Tin mass fraction and isotopic signature of geological reference materials

The applicability of our method for the analysis of natural samples has been assessed with the replicate analyses of ten geological reference materials of different types. The results are reported in Table 5 and Figure 5. These analyses include separate digestions of given rock powders and
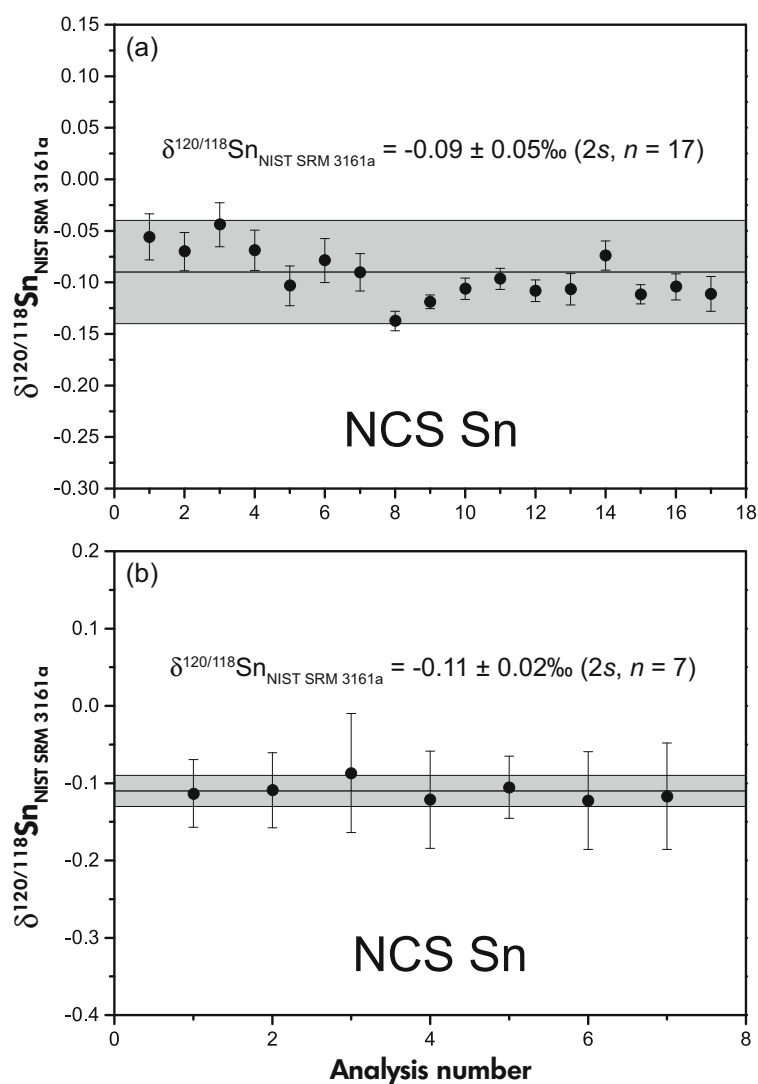
Figure 3. Sn isotopic signature of the standard solution NCS Sn relative to the NIST SRM 3161a. (a) The instrumental mass fractionation was corrected by SSB; (b) the instrumental mass fractionation was corrected by DS. Range bars are the measurement repeatability (2SE), and the measurement repeatability is represented by the grey band (2s).

Figure 4. Results of doping the NIST SRM 3161a reference material at a range mass fraction relative to Sn with several different elements. Range bars represent 2 standard error (2SE) of each measurement. Shaded boxes indicate the intermediate measurement precision (over an extended period; 2s, n = 81) on undoped measurements of NIST SRM 3161a.

duplicate column chemistry using independent solutions of the same sample. Total procedural blanks are < 6 ng. The blank contribution is < 3% sample Sn contents (> 200 ng), thus having no significant effect on the measured Sn isotopic signature of the samples.

The Sn mass fractions of the ten reference materials were determined by the DS technique (Table 5). The RSD (relative standard deviation) of Sn mass fraction results was within 5% for most of the reference materials except for a manganese nodule (NOD-A-1) for which the RSD was as high as 12%. The Sn mass fraction results of the reference materials are generally in agreement with published data where available (Table 5; Axelsson et al. 2002, Dampare et al. 2008,

Hu and Gao 2008, Marx and Kamber 2010, Cotta and Enzweiler 2013, Kon and Hirata 2015, Jochum et al. 2016, Creech et al. 2017). For example, the Sn mass fraction measured for AGV-2 (mean of 2.01 ± 0.14 µg g^{-1}; 2s, n = 5) agrees with the value of 2.24 ± 0.36 µg g^{-1} (2s, n = 21) reported by Marx and Kamber (2010). The Sn mass fraction measured for NOD-A-1 (mean of 3.03 ± 0.75 µg g^{-1}, 2s, n = 7) agrees with the value of 3.00 ± 0.16 µg g^{-1} (2s, n = 4) reported by Axelsson et al. (2002).

Limited data also make it difficult to compare the Sn isotopic fractionation of some geological reference materials between different laboratories. Moreover, the absence of an internationally accepted zero-delta reference material

Table 5.
$\delta^{120/118}Sn_{NIST\ SRM\ 3161a}$ and Sn mass fraction values for different geological reference materials. Relevant literature data are also listed

| Sample	Lithology	Origin	Sn mass fraction (µg g⁻¹)	2s	$\delta^{120/118}Sn$ (2s)	$\delta^{120/118}Sn/amu$ (2s)	n
BHVO-2 (USGS)	Basalt	This Study	1.81	0.02	0.19 ± 0.07	0.10 ± 0.03	6
		Wang et al. (2017)[a]			0.07 ± 0.02	0.03 ± 0.01	2
		Creech et al. (2017)[b]	1.9	0.04	0.32 ± 0.03	0.16 ± 0.02	6
		Jochum et al. (2016)	1.776	0.98			34
W-2a (USGS)	Diabase	This Study	1.84	0.14	0.16 ± 0.05	0.08 ± 0.03	5
		Dampare et al. (2008)	2				
AGV-2 (USGS)	Andesite	This Study	2.01	0.14	0.13 ± 0.03	0.07 ± 0.01	5
		Creech et al. (2017)[b]	2.07		0.25 ± 0.07	0.12 ± 0.03	1
		Marx and Kamber (2010)	2.242	0.36			4
		Jochum et al. (2016)	1.83	2.14			18
JA-2 (GSJ)	Andesite	This Study	1.63	0.27	0.11 ± 0.01	0.06 ± 0.01	6
		Jochum et al. (2016)	1.69	0.44			7
		Kon and Hirata (2015)	1.65	0.44			10
GSP-2 (USGS)	Granodiorite	This Study	6.53	0.36	0.12 ± 0.06	0.06 ± 0.03	6
		Creech et al. (2017)[b]	8.32		0.18 ± 0.03	0.09 ± 0.02	1
		Cotta and Enzweiler (2013)	6.4	0.3			5
JG-2 (GSJ)	Granite	This Study	2.6	0.27	0.22 ± 0.05	0.11 ± 0.03	6
		Kon and Hirata (2015)	2.843	0.056			10
G-2 (USGS)	Granite	This Study	1.75	0.03	0.18 ± 0.05	0.09 ± 0.03	3
		Jochum et al. (2016)	1.72	0.66			8
GBW07316 (NICG)	Marine sediment	This Study	1.68	0.1	0.14 ± 0.02	0.07 ± 0.01	3
NOD-A-1 (USGS)	Marine sediment	This Study	3.03	0.75	0.14 ± 0.02	0.07 ± 0.01	3
		Axelsson et al. (2002)	3	0.16			4
SGR-1 (USGS)	Oil shale	This Study	1.62	0.03	0.14 ± 0.03	0.07 ± 0.02	3
		Hu and Gao (2008)	1.72				
Sn_IPGP	Standard solution	She et al. (2020)[c]			0.09 ± 0.03		35

The repeatability on single measurement is the 2SE (standard error) of the analyses, and where n > 1, data represent the 2s (standard deviations).
n is the number of digestions.

[a] The Sn isotopic signature was represented $\delta^{124/116}Sn$, relative to NIST SRM 3161a, and can be transformed to $\delta^{120/118}Sn$ by multiplying by 1/4.

[b] The Sn isotopic signature was represented $\delta^{122/118}Sn$, relative to Sn_IPGP. The results listed in the table have been converted to $\delta^{120/118}Sn$, relative to NIST SRM 3161a by Equation (2) and a linear fractionation law using data from She et al. (2020), the 2 standard deviation were calculated by standard error propagation.

[c] The Sn isotopic signature was represented $\delta^{120/118}Sn$, relative to NIST SRM 3161a.
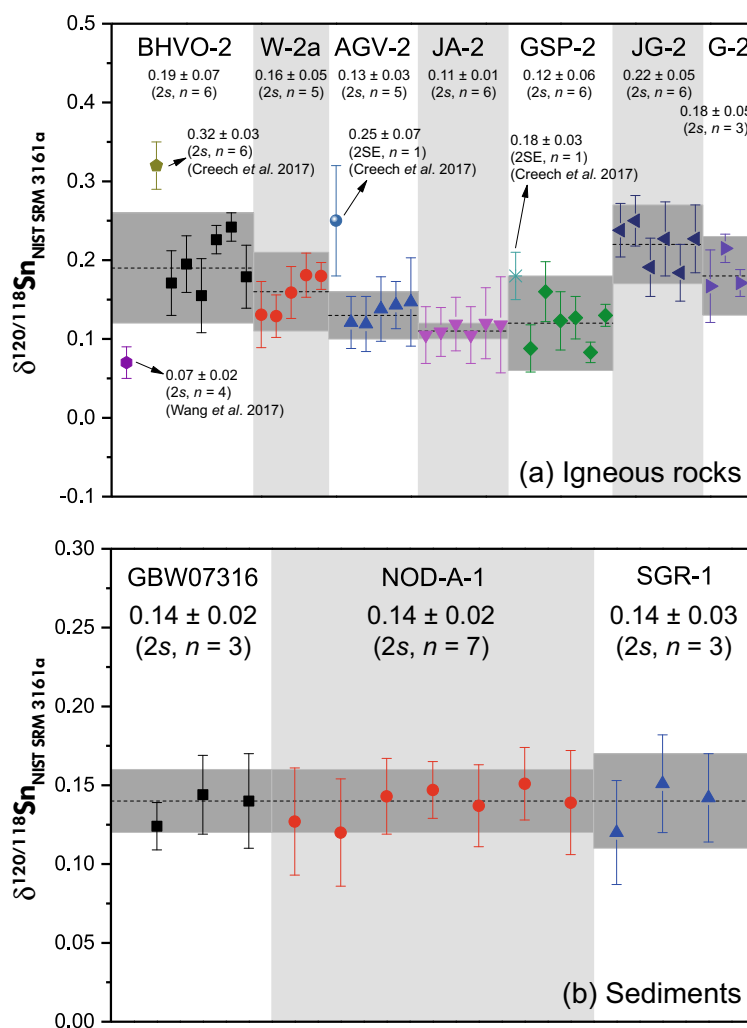
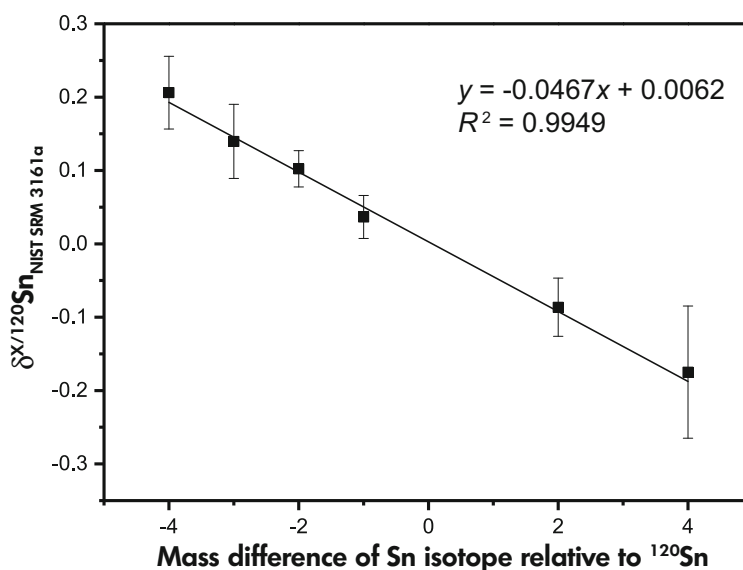**Figure 5.** $\delta^{120/118}$Sn value of (a) igneous rocks and (b) sediments shown with the previously published results. The range bars represents the 2 standard error (2SE). Creech *et al.* (2017) reported the $\delta^{120/118}$Sn data that were re-calibrated to NIST SRM 3161a by the standard conversion identity and the 2 standard deviation were calculated by standard error propagation. The grey area represents 2 standard deviation (2s) of the $\delta^{120/118}$Sn value of the samples. Data are shown in Table 5.

solution has prevented rigorous inter-laboratory comparisons. A recent study of the Sn isotopic signature of four Sn standard solutions (She *et al.* 2020) found that the Sn isotopic signature for the Sn_IPGP and NIST SRM 3161a standard solutions is different from the $\delta^{122/116}$Sn of Sn_IPGP relative to NIST SRM 3161a (Lot 140917) reference material being 0.27 ± 0.09‰ (2s, n = 35).

In this study, the Sn isotopic signatures are expressed as $\delta^{120/118}$Sn$_{NIST\ SRM\ 3161a}$. If the isotope signature follows a linear fractionation law, the $\delta^{122/118}$Sn and $\delta^{124/116}$Sn values can be transformed to the $\delta^{120/118}$Sn by multiplying by 1/2 and 1/4, respectively. Wombacher and

Rehkämper (2004) reported that there are slight differences in per amu between the results from the isotopic signature of different Cd isotope ratios. But if the isotopic variations do not significantly exceed 1‰ amu⁻¹, the effect is neglected given the uncertainties reported here. Creech *et al.* (2017) and Wang *et al.* (2017) reported Sn isotopic variations of < 1‰ amu⁻¹ of the rock reference materials. In addition, the Sn isotopic signature of the standard solution of Sn NCS relatively to NIST 3161a was determined by MC-ICP-MS with SSB to correct for the instrumental mass fractionation. The results showed that the correlation between the mass difference of Sn and the Sn isotopic signature of the Sn NCS follows a linear fractionation law (Figure 6). Thus, the

© 2022 The Authors. Geostandards and Geoanalytical Research © 2022 International Association of Geoanalysts.

Figure 6. Linear relationship between the mass difference of Sn (relative to ^{120}Sn) and the Sn isotopic signature of standard solution NCS Sn relative to the NIST SRM 3161a and the vertical bars represent 2 standard deviation (2s, n = 5).

$\delta^{122/118}$Sn and $\delta^{124/116}$Sn values are transformed to the $\delta^{120/118}$Sn by linear fractionation law.

All Sn isotopic signatures reported in this study are relative to NIST SRM 3161a, which was chosen as the zero-delta reference solution. Other Sn standard solutions (such as Sn_IPGP) can be re-calibrated to NIST SRM 3161a by the standard conversion identity (Vogl and Pritzkow 2010, Goldberg et al. 2013):

$$\delta^{120/118}\text{Sn}_{\text{S-NIST SRM 3161a}} = \delta^{120/118}\text{Sn}_{\text{S-Sn\_IPGP}}$$
$$+ \delta^{120/118}\text{Sn}_{\text{Sn\_IPGP-NIST SRM 3161a}}$$
$$+ \left(\delta^{120/118}\text{Sn}_{\text{S-Sn\_IPGP}} \right.$$
$$\left. \times \delta^{120/118}\text{Sn}_{\text{Sn\_IPGP-NIST SRM 3161a}} \right)$$
$$\times 10^{-3} \tag{2}$$

where $\delta^{120/118}\text{Sn}_{\text{S-NIST SRM 3161a}}$ and $\delta^{120/118}\text{Sn}_{\text{S-Sn\_IPGP}}$ are the Sn isotopic compositions of the sample relative to NIST SRM 3161a and Sn_IPGP, respectively, and $\delta^{120/118}\text{Sn}_{\text{Sn\_IPGP-NIST SRM 3161a}}$ is the Sn isotopic composition of Sn_IPGP relative to the NIST SRM 3161a as reported by She et al. (2020) (Table 5). This conversion assumes that different lots of the same standard solution have the same isotopic composition.

The Sn isotopic signature for BHVO-2 has been determined in previous studies by MC-ICP-MS. Wang

et al. (2017) employed the DS technique and obtained a $\delta^{124/116}$Sn $_{\text{NIST SRM 3161a}}$ value of 0.27 ± 0.06‰ (2s, n = 4) which was transformed to $\delta^{120/118}$Sn $_{\text{NIST SRM 3161a}}$ as 0.07 ± 0.02‰ by multiplying 1/4 (Table 5). Creech et al. (2017) also reported the Sn isotopic signature of BHVO-2 as $\delta^{122/118}$Sn relative to the Sn_IPGP standard solution to be 0.452 ± 0.027‰ (2s, n = 6) which can be converted by standard conversion identity and multiplying 1/2 to $\delta^{120/118}$Sn $_{\text{NIST SRM 3161a}}$ as 0.32 ± 0.03‰ (2s, n = 6; with standard deviation calculated using standard error propagation). These published $\delta^{120/118}$Sn $_{\text{NIST SRM 3161a}}$ results for BHVO-2 are slightly different from each other, ranging from 0.07 to 0.32‰ (Figure 5).

The $\delta^{120/118}$Sn $_{\text{NIST SRM 3161a}}$ value for BHVO-2 is 0.19 ± 0.07‰ (2s, n = 6) which is slightly different from, but within the range of, the published values of 0.07 to 0.32‰. This variance in $\delta^{120/118}$Sn $_{\text{NIST SRM 3161a}}$ values of BHVO-2 is up to 0.25‰ and may be due to the insufficient replication of independent digestions, or the heterogeneity of the BHVO-2. More studies are required to determine how to achieve higher accuracy.

The $\delta^{120/118}$Sn $_{\text{NIST SRM 3161a}}$ results for the AGV-2 and GSP-2 reference materials are 0.13 ± 0.03‰ (2s, n = 5) and 0.12 ± 0.06‰ (2s, n = 6), respectively (Table 5). The $\delta^{122/118}$Sn relative to the Sn_IPGP of AGV-2 and GSP-2 were also determined by Creech et al. (2017) to be 0.310 ± 0.120‰ (2SE, n = 1) and 0.180 ± 0.022‰

(2SE, $n = 1$), respectively. These data are transformed to be $\delta^{120/118}Sn_{NIST\ SRM\ 3161a}$ of $0.25 \pm 0.07\permil$ (2SE, $n = 1$) for AVG-2 and $0.18 \pm 0.03\permil$ (2SE, $n = 1$) for GSP-2, respectively. The reported result for AGV-2 is slightly higher than the value from this study, whereas the reported result for GSP-2 is in agreement with the value from this study, which is within the uncertainty range (Figure 5). Considering that the data reported for AGV-2 and GSP-2 by Creech *et al.* (2017) are only single measurements, the repeat Sn isotopic values for the two reference materials in this study could be more accurate and more representative.

$\delta^{122/118}Sn_{Sn\_IPGP}$ can converted to $\delta^{120/118}Sn_{NIST\ SRM\ 3161a}$ by standard conversion identity. This conversion assumes that different lots of the same standard solution have the same isotopic composition. Compared with our results, Creech *et al.* (2017) reported generally heavier Sn isotopic compositions of three reference materials. This may be due to the use of different lots of the Sn_IPGP standard solution by She *et al.* (2020) and Creech *et al.* (2017). The Sn_IPGP standard solutions may have different isotopic compositions.

We also report the Sn isotopic signature of the W-2a, JA-2, JG-2 and G-2 igneous rocks for the first time (Table 5). The $\delta^{120/118}Sn_{NIST\ SRM\ 3161a}$ values for these four reference materials vary slightly from $0.11\permil$ to $0.22\permil$ (Table 5 and Figure 5). The Sn isotopic signature was also analysed for a marine sediment (GBW07316), a manganese nodule (NOD-A-1) and an oil shale (SGR-1). These samples are enriched in heavy Sn isotopes relative to NIST SRM 3161a with the $\delta^{120/118}Sn_{NIST\ SRM\ 3161a}$ values of $0.14 \pm 0.02\permil$ (2s, $n = 3$), $0.14 \pm 0.02\permil$ (2s, $n = 7$) and $0.14 \pm 0.03\permil$ (2s, $n = 3$), respectively (Table 5; Figure 5). The indistinguishable Sn isotopic signature of the marine sediments may indicate that there is no mass fractionation during Sn adsorption or precipitation from seawater to sediments under different redox conditions. Nevertheless, there are no data to refer to for the Sn isotopic signature of seawater, and thus, further studies are required to confirm this finding.

The ^{116}Sn-^{117}Sn-^{119}Sn-^{120}Sn are also used for the DS inversion. The results show that the $\delta^{120/116}Sn\ amu^{-1}$ and $\delta^{120/118}Sn\ amu^{-1}$ of most of the reference materials are consistent considering the error ranges except for the sedimentary samples which are different and have a poorer precision (Table S2). This may be caused by some potential isobaric interference and/or matrix effect. Therefore, it is better to use $\delta^{120/118}Sn$ to represent the isotopic compositions of Sn.

Overall, the results from these tests of NIST SRM 3161a and geological reference materials demonstrate that Sn

isotopes can be measured, with a precision of $\pm 0.07\permil$ (2s) for $\delta^{120/118}Sn_{NIST\ SRM\ 3161a}$ based on repeated analyses of BHVO-2. The precision is at the same level as the precision of the reported data. These data provide a basis for quality assurance and inter-laboratory comparisons of high-precision Sn isotopic data.

Conclusions

The procedure adopted using the AG MP-1 and TRU-Spec resins can separate Sn from the matrix elements in common geological materials effectively. The ^{117}Sn-^{119}Sn DS technique and MC-ICP-MS were conducted to measure Sn isotopic signatures. Precisions of $\pm 0.03\permil$ (2s) and $\pm 0.07\permil$ (2s) were obtained for the $\delta^{120/118}Sn_{NIST\ SRM\ 3161a}$ of the NIST SRM 3161a and BHVO-2, respectively. Analyses of ten different reference materials demonstrate that the method can be effectively applied to a wide range of geological materials. The results of the Sn isotopic signature are suitable for sample calibration and lay the foundation for quality assurance and inter-laboratory comparison.

Acknowledgements

Data availability statement

The data that support the findings of this study are openly available in GeoReM at http://georem.mpch-mainz.gwdg.de.

References

Albarède F. and Beard B. (2004)
Analytical methods for non-traditional isotopes. In: Johnson C.M., Beard B.L. and Albarède F. (eds), Geochemistry of non-traditional stable isotopes. Mineralogical Society of America and Geochemical Society (Chantilly), 113–152.

Axelsson M.D., Rodushkin I., Ingri J. and Ohlander B. (2002)
Multielemental analysis of Mn-Fe nodules by ICP-MS: Optimisation of analytical method. **Analyst, 127,** 76–82.

Badullovich N., Moynier F., Creech J., Teng F.Z. and Sossi P.A. (2017)
Tin isotopic fractionation during igneous differentiation and Earth's mantle composition. Geochemical Perspectives Letters, 5, 24–28.

Balliana E., Aramendia M., Resano M., Barbante C. and Vanhaecke F. (2013)
Copper and tin isotopic analysis of ancient bronzes for archaeological investigation: Development and validation of a suitable analytical methodology. Analytical and Bioanalytical Chemistry, 405, 2973–2986.

Berger D., Figueiredo E., Brügmann G. and Pernicka E. (2018)
Tin isotope fractionation during experimental cassiterite smelting and its implication for tracing the tin sources of prehistoric metal artefacts. Journal of Archaeological Science, 92, 73–86.

Brügmann G., Berger D. and Pernicka E. (2017)
Determination of the tin stable isotopic composition in tin-bearing metals and minerals by MC-ICP-MS. Geostandards and Geoanalytical Research, 41, 437–448.

Cheng T., Nebel O., Sossi P.A. and Chen F. (2014)
Refined separation of combined Fe-Hf from rock matrices for isotope analyses using AG-MP-1M and ln-spec chromatographic extraction resins. MethodsX, 1, 144–150.

Clayton R., Andersson P., Gale N.H., Gillis C. and Whitehouse M.J. (2002)
Precise determination of the isotopic composition of Sn using MC-ICP-MS. Journal of Analytical Atomic Spectrometry, 17, 1248–1256.

Cotta A.J.B. and Enzweiler J. (2013)
Determination of Cr, Cu, Ni, Sn, Sr and Zn mass fractions in geochemical reference materials by isotope dilution ICP-MS. Geostandards and Geoanalytical Research, 37, 35–50.

Creech J.B. and Moynier F. (2019)
Tin and zinc stable isotope characterisation of chondrites and implications for early solar system evolution. Chemical Geology, 511, 81–90.

Creech J.B., Moynier F. and Badullovich N. (2017)
Tin stable isotope analysis of geological materials by double-spike MC-ICP-MS. Chemical Geology, 457, 61–67.

Creech J.B., Moynier F. and Koeberl C. (2019)
Volatile loss under a diffusion-limited regime in tektites: Evidence from tin stable isotopes. Chemical Geology, 528, 119279.

Dampare S.B., Shibata T., Asiedu D.K., Osae S. and Banoeng-Yakubo B. (2008)
Geochemistry of Paleoproterozoic metavolcanic rocks from the southern Ashanti volcanic belt, Ghana: Petrogenetic and tectonic setting implications. Precambrian Research, 162, 403–423.

de Laeter J.R. and Jeffery P.M. (1965)
The isotopic composition of terrestrial and meteoritic tin. Journal of Geophysical Research, 70, 2895–2903.

de Laeter J.R. and Jeffery P.M. (1967)
Tin: Its isotopic and elemental abundance. Geochimica et Cosmochimica Acta, 31, 969–985.

Dodson M.H. (1963)
A theoretical study of the use of internal standards for precise isotopic analysis by the surface ionization technique: Part I – General first-order algebraic solutions. Journal of Scientific Instruments, 40, 289–295.

Encinar J.R., Gonzalez P.R., Alonso J.I.G. and Sanz-Medel A. (2002)
Evaluation of extraction techniques for the determination of butyltin compounds in sediments using isotope dilution-GC/ICP-MS with ^{118}Sn and ^{119}Sn-enriched species. Analytical Chemistry, 74, 270–281.

Eugster O., Tera F. and Wasserburg G.J. (1969)
Isotopic analyses of barium in meteorites and in terrestrial samples. Journal of Geophysical Research, 74, 3897–3908.

Fehr M.A., Rehkämper M. and Halliday A.N. (2004)
Application of MC-ICP-MS to the precise determination of tellurium isotope compositions in chondrites, iron meteorites and sulfides. International Journal of Mass Spectrometry, 232, 83–94.

Friebel M., Toth E.R., Fehr M.A. and Schönbächler M. (2020)
Efficient separation and high-precision analyses of tin and cadmium isotopes in geological materials. Journal of Analytical Atomic Spectrometry, 35, 273–292.

Goldberg T., Gordon G., Izon G., Archer C., Pearce C.R., McManus J., Anbar A.D. and Rehkämper M. (2013)
Resolution of inter-laboratory discrepancies in Mo isotope data: An intercalibration. Journal of Analytical Atomic Spectrometry, 28, 724–735.

Haustein M., Gillis C. and Pernicka E. (2010)
Tin isotopy – A new method for solving old questions. Archaeometry, 52, 816–832.

Hu J.Y. and Dauphas N. (2017)
Double-spike data reduction in the presence of isotopic anomalies. Journal of Analytical Atomic Spectrometry, 32, 2024–2033.

Hu Z. and Gao S. (2008)
Upper crustal abundances of trace elements: A revision and update. Chemical Geology, 253, 205–221.

Jochum K.P., Weis U., Schwager B., Stoll B., Wilson S.A., Haug G.H., Andreae M.O. and Enzweiler J. (2016)
Reference values following ISO guidelines for frequently requested rock reference materials. Geostandards and Geoanalytical Research, 40, 333–350.

Kon Y. and Hirata T. (2015)
Determination of 10 major and 34 trace elements in 34 GSJ geochemical reference samples using femtosecond laser ablation ICP-MS. Geochemical Journal, 49, 351–375.

Lamboux A., Hassler A., Davechand P. and Balter V. (2020)
Absence of temperature effect on elution profiles on anionic and cationic ion-exchange resins from 4 °C to 28 °C. Rapid Communications in Mass Spectrometry, 34, e8806.

Malinovskiy D., Moens L. and Vanhaecke F. (2009)
Isotopic fractionation of Sn during methylation and demethylation reactions in aqueous solution. Environmental Science and Technology, 43, 4399–4404.

Marx S.K. and Kamber B.S. (2010)
Trace-element systematics of sediments in the Murray-Darling basin, Australia: Sediment provenance and palaeoclimate implications of fine scale chemical heterogeneity. Applied Geochemistry, 25, 1221–1237.

Mason A., Powell W., Bankoff H.A., Mathur R., Price M., Bulatovic A. and Filipovic V. (2020)
Provenance of tin in the late bronze age Balkans based on probabilistic and spatial analysis of Sn isotopes. Journal of Archaeological Science, 122, 105181.

McNaughton N. and Rosman K.J.R. (1991)
Tin isotope fractionation in terrestrial cassiterites. Geochimica et Cosmochimica Acta, 55, 499–504.

Nickel D., Haustein M., Lampke T. and Pernicka E. (2012)
Identification of forgeries by measuring tin isotopes in corroded bronze objects. Archaeometry, 54, 167–174.

Qu Q., Liu G., Henry M., Point D., Chmeleff J., Sun R., Sonke J.E. and Chen J. (2020)
Tin stable isotopes in magmatic-affected coal deposits: Insights in the geochemical behavior of tin. Applied Geochemistry, 119, 104641.

Rosman K.J.R. and McNaughton N.J. (1987)
High-precision measurement of isotopic fractionation in tin. International Journal of Mass Spectrometry and Ion Processes, 75, 91–98.

Rosman K.J.R. and Taylor P.D.P. (1998)
Isotopic compositions of the elements 1997. Pure and Applied Chemistry, 70, 217–235.

Rudge J.F., Reynolds B.C. and Bourdon B. (2009)
The double spike toolbox. Chemical Geology, 265, 420–431.

Russell W.A., Papanastassiou D.A. and Tombrello T.A. (1978)
Ca isotope fractionation on the earth system materials and other solar system materials. Geochimica et Cosmochimica Acta, 42, 1075–1090.

Schulze M., Ziegerick M., Horn I., Weyer S. and Vogt C. (2017)
Determination of tin isotope ratios in cassiterite by femtosecond laser ablation multicollector inductively

coupled plasma-mass spectrometry. Spectrochimica Acta Part B, 130, 26–34.

She J.-X., Wang T., Liang H., Muhtar M.N., Li W. and Liu X. (2020)
Sn isotope fractionation during volatilization of Sn(IV) chloride: Laboratory experiments and quantum mechanical calculations. Geochimica et Cosmochimica Acta, 269, 184–202.

Sun J., Zhu X., Tang S. and Chen Y. (2012)
Investigation of matrix effects in the MC-ICP-MS induced by Nb, W and Cu: Isotopic case studies of iron and copper. Chinese Journal of Geochemistry, 32, 1–6.

van der Walt T.N. and Coetzee P.P. (1996)
Behaviour of Mo, Al, As, Cs, Sn, Sb, Pd, Rh, Ru, Ge, Se and Te on the macroporous resin AG MP-1 in alkaline medium. Fresenius' Journal of Analytical Chemistry, 356, 425–429.

Vogl J. and Pritzkow W. (2010)
Isotope reference materials for present and future isotope research. Journal of Analytical Atomic Spectrometry, 25, 923–932.

Wang X., Amet Q., Fitoussi C. and Bourdon B. (2018)
Tin isotope fractionation during magmatic processes and the isotope composition of the bulk silicate earth. Geochimica et Cosmochimica Acta, 228, 320–335.

Wang X., Fitoussi C., Bourdon B. and Amet Q. (2017)
A new method of Sn purification and isotopic determination with a double-spike technique for geological and cosmochemical samples. Journal of Analytical Atomic Spectrometry, 32, 1009–1019.

Wang X., Fitoussi C., Bourdon B.F. Jr. and Charnoz S. (2019)
Tin isotopes indicative of liquid-vapour equilibration and separation in the moon-forming disk. Nature Geoscience, 12, 707–711.

Wombacher F. and Rehkämper M. (2004)
Problems and suggestions concerning the notation of cadmium stable isotope compositions and the use of reference materials. Geostandards and Geoanalytical Research, 28, 173–178.

Yamazaki E., Nakai S., Sahoo Y., Yokoyama T., Mifune H., Saito T., Chen J., Takagi N., Hokanishi N. and Yasuda A. (2014)
Feasibility studies of Sn isotope composition for provenancing ancient bronzes. Journal of Archaeological Science, 52, 458–467.

Yamazaki E., Nakai S.I., Yokoyama T., Ishihara S. and Tang H. (2013)
Tin istope analysis of cassiterites from southeastern and eastern Asia. Geochemical Journal, 47, 21–35.

Yao J., Mathur R., Powell W., Lehmann B., Tornos F., Wilson M. and Ruiz J. (2018)
Sn-isotope fractionation as a record of hydrothermal redox reactions. American Mineralogist, 103, 1591–1598.

Yi W., Halliday A.N., Lee D.C. and Christensen J.N. (1995)
Indium and tin in basalts, sulfides and the mantle.
Geochimica et Cosmochimica Acta, 59, 5081–5090.

Zhang L., Li J., Xu Y.-G. and Ren Z.-Y. (2018)
The influence of the double spike proportion effect on stable isotope (Zn, Mo, Cd and Sn) measurements by multicollector-inductively coupled plasma-mass spectrometry (MC-ICP-MS). Journal of Analytical Atomic Spectrometry, 33, 555–562.

Zhang L., Ren Z.-Y., Xia X.-P., Li J. and Zhang Z.-F. (2015)
IsotopeMaker: A Matlab program for isotopic data reduction. International Journal of Mass Spectrometry, 392, 118–124.

Supporting information

The following supporting information may be found in the online version of this article:

Figure S1. Contour plot of error in α for (a) the ^{117}Sn-^{119}Sn DS and (b) ^{117}Sn-^{112}Sn DS, with ^{117}Sn-^{118}Sn-^{119}Sn-^{120}Sn and ^{117}Sn-^{118}Sn-^{120}Sn-^{122}Sn inversion, respectively.

Table S1. The polyatomic interference on Sn isotopes.

Table S2. $\delta^{120/116}$Sn$_{NIST\ SRM\ 3161a}$ value for different geological reference materials.

This material is available from: http://onlinelibrary.wiley.com/doi/10.1111/ggr.12443/abstract (This link will take you to the article abstract).